

Chapter 19

Dynamic Light Scattering with Nanoparticles: Setup and Preliminary Results

G. Derkachov, D. Jakubczyk, K. Kolwas, Y. Shopa, and M. Woźniak

19.1 Experimental Method and DLS Setup

Dynamic light scattering (DLS) method for particle size determination is based on the measurement of scattered light intensity fluctuations on a micro- and millisecond time scale in a volume containing particles in suspension or solution [1–3]. The motion of particles is diffusion controlled and is characterized by the diffusion coefficient D . For noninteracting spherical Brownian particles in suspension characterized with a low Reynolds number, the Stokes-Einstein equation holds:

$$D = \frac{kT}{6\pi\eta R_h}, \quad (19.1)$$

where R_h is the so-called hydrodynamic radius, η is the dynamic viscosity of the dispersion medium, T is the absolute temperature, and k is the Boltzmann constant. The obtained optical signal shows random changes due to the Brownian motions of the particles. This signal can be interpreted in terms of an autocorrelation function (ACF). Incoming signal is processed in real time with a digital correlator, and the ACF versus the delay time τ is extracted. Time-dependent autocorrelation function

G. Derkachov • D. Jakubczyk • K. Kolwas • M. Woźniak
Institute of Physics, Polish Academy of Sciences, Aleja Lotników 32/46, PL-02668,
Warsaw, Poland
e-mail: derkaczg@ifpan.edu.pl

Y. Shopa (✉)
Cardinal Stefan Wyszyński University in Warsaw, ul. Dewajtis 5, PL-01815, Warsaw, Poland
e-mail: i.shopa@uksw.edu.pl

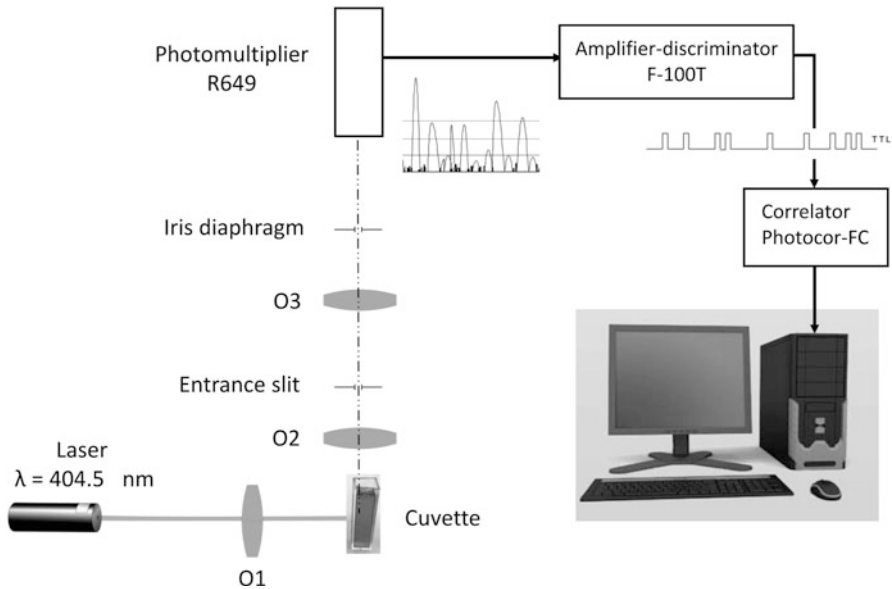


Fig. 19.1 Schematic diagram of the DLS experimental setup

$G(\tau)$, which is measured experimentally, typically is decaying exponentially with a decay constant Γ

$$G(\tau) = B_0 + B_1 \exp(-2\Gamma\tau), \quad (19.2)$$

where B_0 and B_1 are constants independent of time. In such case, after processing the experimental data, the diffusion coefficient D can be found from $\Gamma = Dq^2$ relation, where $q = \frac{4\pi}{\lambda} n \sin(\theta/2)$ is the scattering number, θ is the angle between the incident and the scattered light wave vectors, and n is the refractive index. Inserting D into the Stokes-Einstein equation (19.1) yields the particle size.

The schematic diagram of the experimental setup for DLS measurements is presented in Fig. 19.1. As the light source we chose 404.5 nm laser with 22 mW output power, because violet light gives higher scattering intensity than the more commonly used red. Laser light passes through a 60-mm focal range lens that focuses the beam into the cell with the investigated liquid placed in the temperature-stabilized cylindrical jacket. In order to minimize the effect of stray light and maximize the signal to noise ratio, the scattered light is collected at $\theta = 90^\circ$ to the incident beam with a confocal lens system and fed into a photomultiplier tube (Hamamatsu R649 in a C10372 dedicated housing).

The signal from the photomultiplier is converted with transimpedance preamplifier/discriminator (Advanced Research Instruments Corporation, F-100T) to TTL level 10-ns pulses and sent to real-time correlator (Photocor-FC) built with a software-configurable FPGA circuits [4]. The DLS setup (with a single photomulti-

plier) outputs the count rate and the autocorrelation function. The results are stored in an ASCII data file and analyzed with Alango DynaLS software [5–7].

In order to find ACF reliably, the signal must be measured over a relatively long time (>60 s). The scattered light intensity (count rate) depends on the number of particles diffusing within the sample volume. The dark current pulses in our experiments did not exceed 150 cps level.

19.2 DLS Setup Calibration with Gold and Silicon Dioxide Nanoparticles

First DLS measurements were performed with ultrapure water suspensions of highly monodisperse gold and SiO₂ spheres with diameters of 30 and 445 nm, respectively. The samples were loaded into a 3-mL cuvette with 10-mm square cross section.

The measurements of ACF of monodisperse gold particles with a diameter of 30 nm (given by the manufacturer) show single exponential decay with the relaxation time $1/2\Gamma = \tau_0 = 0.068$ ms (Fig. 19.2). Using the physical parameters of the experiment, we obtained the nanoparticles diameter of 30.8 nm, which is in good agreement with the value given by the manufacturer. DLS measurement of SiO₂ spheres in water gives 1.16 ms and 452 nm, which is also in agreement with the diameter given by the manufacturer. In case of monodisperse particles, the hydrodynamic diameter DLS measurement error does not exceed several percent.

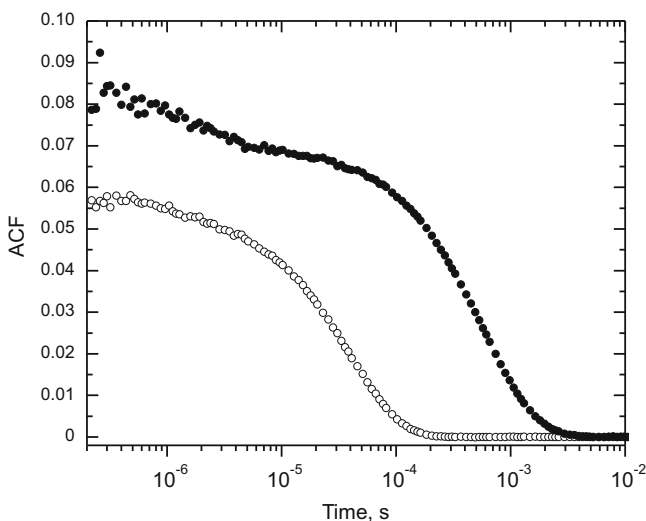


Fig. 19.2 The measured ACF for 30 nm gold (\circ) and 445 nm SiO₂ (\bullet) particles in water

The presented measurements indicate that our setup was properly calibrated and that it should produce reliable results.

19.3 Study of Aqueous Solutions of Sodium Dodecyl Sulfate

Our further studies were focused on sodium dodecyl sulfate (SDS), a synthetic organic compound with the formula of $\text{CH}_3(\text{CH}_2)_{11}\text{SO}_4\text{Na}$. We have measured dynamic light scattering on aqueous solutions of SDS as a function of SDS concentration and temperature. Samples were prepared from commercial SDS product (Sigma-Aldrich, ACS reagent, $\geq 99.0\%$) with ultrapure water produced in-lab (Millipore, Simplicity UV) few day before the experiments, with concentrations of 5, 12, 20, 30, 40, 60, 80, and 100 mM/L. On loading into the cuvette, a 0.2-micron filter was used. The temperature was stabilized down to ± 0.5 K in 295–340 K range.

In order to calculate R_h from the Stokes-Einstein equation, the refractive index of dispersion medium/solvent and its viscosity must be known. The refractive index of 100 mM/L SDS solution differs by less than 0.001 from that of pure water. Thus for finding q we used the n value for water and its respective temperature dispersion from [8] and [9]. Considering the low SDS concentration, the dynamic viscosity η and its temperature dependence were also taken for pure water.

For the SDS solution concentrations used in experiment, the measured scattered light intensities were exceptionally small: from 5000 to 50,000 cps. In consequence, obtaining an ACF suitable for interpretation required long accumulation times. We found that SDS formed relatively very large, non-spherical aggregates in water [10–12], which manifested in ACF (Fig. 19.3) as a slope around 400 ms. Filtering did not remove these SDS aggregates. They weakly depended on SDS concentration, while they seemed to diminish with growing temperature. Due to high non-sphericity calculating of hydrodynamic radius made no sense.

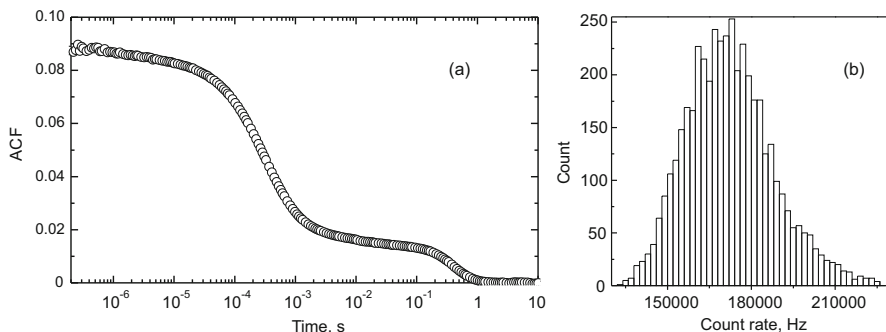


Fig. 19.3 Results from dynamic light scattering experiments on 12 mM/L SDS solution, which shows high values of correlation time. The corresponding count rate histogram exhibits a classical gaussian-like shape

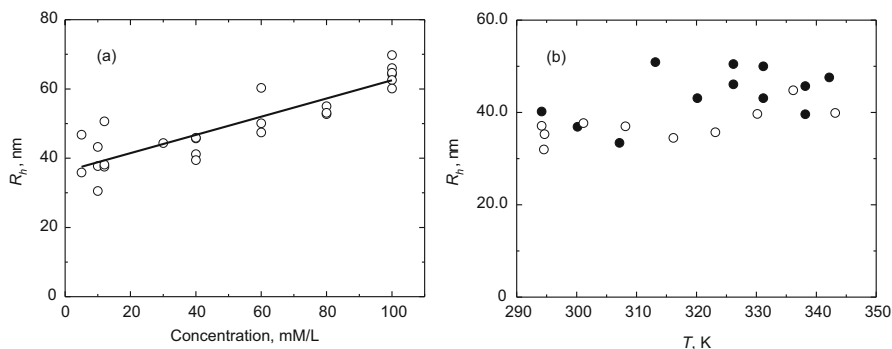


Fig. 19.4 Hydrodynamic radius R_h as a function of SDS concentration in water (a) and as a function of temperature (b) for concentrations of 12 (○) and 20 mM/L (●)

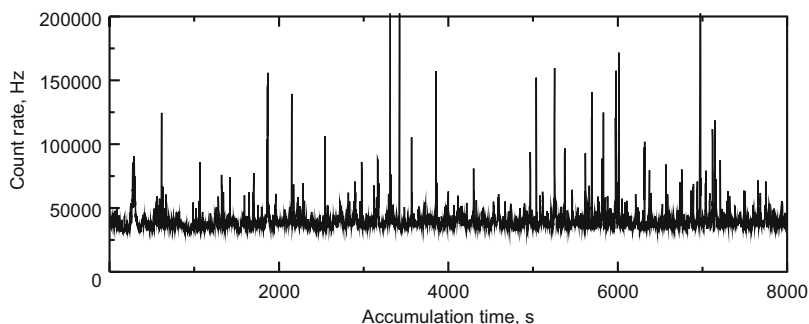


Fig. 19.5 Count rate monitor for 20 mM/L SDS concentration, at 295.5 K and 8000 s accumulation time

On the other hand, the relaxation time of ~ 0.3 ms would correspond to aggregates of several dozen nanometers in size, which is much larger than the micelle size [13, 14]. Their size depended on the SDS concentration; however, we did not observe any phase transition versus the concentration. The corresponding relaxation time depended on the temperature, but due to the opposite temperature dependence of D , the aggregate size hardly exhibited any temperature dependence. Both dependencies – versus concentration and versus temperature – are shown in Fig. 19.4.

Count rate monitor shown in Fig. 19.5 exhibits short-lasting high-value intensity deviations from the average scattering intensity of a long measurement. It seems to indicate the presence of ultra-large aggregates in the SDS solution, which scatter light very intensively. Such scattering episodes preclude accessing short relaxation times in the correlation function.

19.4 First ACF of the Single Droplet

Our ultimate goal is the application of DLS to single, freely suspended multi-component droplets. Our preliminary experimental results confirm the possibility of such DLS usage.

We applied the DLS technique to single droplets levitated in an electrodynamic quadrupole trap. Electrodynamic trapping is a well-established experimental technique [15–17] using a combination of alternating (AC) and static (DC) electric fields to constrain particle to a small volume, ideally to a point. The droplet was illuminated with 458-nm vertically polarized Ar⁺ laser light, and the scattered light was collected around the right angle in the horizontal scattering plane. The droplet was in the focus of an objective, and the collected light was introduced into an optical fiber and fed to a photomultiplier. For higher scattered light intensity, the scattered light might also be collected directly into an optical fiber. Using an optical fiber for the collection of scattered light (in the Mie regime) has an advantage over a lens optics [18, 19] since the fiber entrance aperture works as a good spatial filter and ensures a small area of coherence which is important for ACF quality.

In experiments presented in this work, we used several micron-sized droplets of pure diethylene glycol in a dry nitrogen atmosphere. An example of ACF obtained with the described method is presented in Fig. 19.6.

The first results were obtained within a 30-s interval, which was found sufficient to calculate the ACF. Due to the evaporation of the droplet, there is a decrease of the scattered light intensity, and the collection interval must be appropriately short in order to obtain a sensible ACF. However, the amplitude of ACF was very large in comparison to the results obtained for a bulk solution/suspension in a cuvette.

We expect that, in general, characteristic times found from ACF can be attributed to different phenomena associated with the droplet, for instance, macro- and

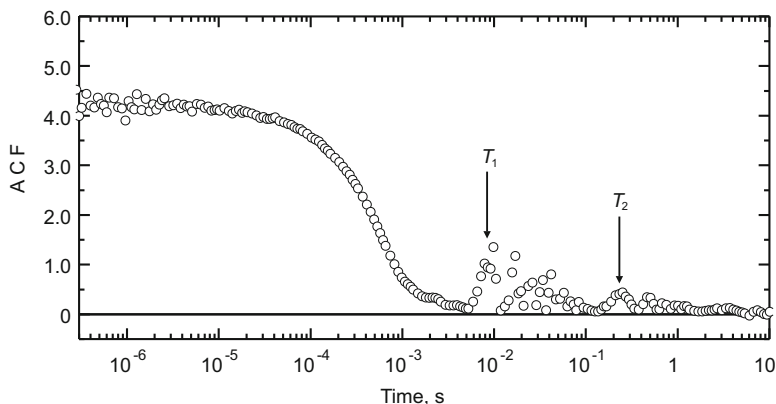


Fig. 19.6 The measured correlation function for a pure diethylene glycol droplet. Characteristic times $T_1 = 8.4$ ms and $T_2 = 0.23$ s of droplet motion are indicated with arrows

micromotion of the droplet in the trap and rotations of the droplet. For a droplet of suspension, the motions of particles inside the droplet should be visible as well, since their characteristic time is much different from the mentioned above. For a droplet of a pure liquid (diethylene glycol) and the light collection with the lens, the micromotion of the droplet with the drive frequency of the trap at 120 Hz was plainly visible (Fig. 19.6). The second type of droplet motion at 4.3 Hz could be possibly associated with the secular (macro) motion in the trap.

19.5 Conclusions

The DLS setup was designed, built, and used for studying diverse solutions and suspensions of nanoparticles. It was tested with bulk gold and silica nanosuspensions in a cuvette and produced good results. Next, we tried to apply the DLS method to sodium dodecyl sulfate solution in cuvette versus temperature and SDS concentration. We found aggregates of various sizes and probably complex morphology. However, the interpretation of the results in detail seems hardly possible. In general, the preliminary results showed that the sensitivity of the DLS setup is sufficient for detection of light scattered by a single micron-sized droplet. We started our experiments with droplets of diethylene glycol and obtained an ACF exhibiting at least two characteristic times, corresponding to motions of the droplet in the trap. We expect that for a droplet of suspension, there is a possibility to find characteristic times corresponding to the evolution of suspension in the droplet and its internal structure.

Acknowledgements The authors acknowledge financial support from the National Science Centre, Poland, grants number 2014/13/D/ST3/01882 and 2014/13/B/ST3/04414.

References

1. Chu B (1974) *Laser light scattering*. Academic Press, New York
2. Brown W (1993) *Dynamic light scattering: the method and some applications*. Oxford University Press, New York
3. Frisken BJ (2001) Revisiting the method of cumulants for the analysis of dynamic light scattering data. *Appl Opt* 40:4087–4091
4. Multi-angle dynamic and static light scattering instrument Photocor complex. www.photocor.com. Cited 7 Dec 2016
5. Koppel DE (1972) Analysis of macromolecular polydispersity in intensity correlation spectroscopy: the method of cumulants. *J Chem Phys* 57:4814–4820
6. Provencher SW (1979) Inverse problems in polymer characterization: direct analysis of polydispersity with photon correlation spectroscopy. *Macromol Chem Phys* 180:201–209
7. Software for particle size distribution analysis in photon correlation spectroscopy. <http://www.softscientific.com/science/WhitePapers/dynals1/dynals100.htm>. Cited 12 Dec 2016

8. Harvey AH, Gallagher JS, Levelt Sangers JMH (1998) Revised formulation for the refractive index of water and steam as function of wavelength, temperature and density. *J Phys Chem Ref Data* 27:761–775
9. Bashkatov AN, Genina EA (2003) Water refractive index in dependence on temperature and wavelength: a simple approximation. *Proc SPIE* 5068:393–395
10. Hayashi S, Ikeda S (1980) Micelle size and shape of sodium dodecyl sulfate in concentrated sodium chloride solutions. *J Phys Chem* 84:744–751
11. Ikeda S, Hayashi S, Imae T (1981) Rodlike micelles of sodium dodecyl sulfate in concentrated sodium halide solutions. *J Phys Chem* 85:106–112
12. Almgren M, Swarup S (1982) Size of sodium dodecyl sulfate micelles in the presence of additives. 2. Aromatic and saturated hydrocarbons. *J Phys Chem* 86:4212–4216
13. Mukerjee P, Mysels KJ (1971) Critical micelle concentration of aqueous surfactant systems. NSRDS-NBS series, vol 36. U.S. National Bureau of Standards, Washington, DC
14. Kenneth G, Norelus A (1993) Determining the critical micelle concentration of aqueous surfactant solutions: using a novel colorimetric method. *J Chem Educ* 70:254–257
15. Woźniak M, Derkachov G, Kolwas K, Archer J, Wojciechowski T, Jakubczyk D, Kolwas M (2015) Formation of highly ordered spherical aggregates from drying microdroplets of colloidal suspension. *Langmuir* 31(28):7860–7868
16. Major F, Gheorghe V, Werth G (2005) Charged particle traps. Springer, Berlin
17. Arnold S (1991) A three-axis spherical void electrodynamic levitator trap for micro-particle experiments. *Rev Sci Instrum* 62:3025–3028
18. MacFadyen AJ, Jennings BR (1990) Fibre-optic systems for dynamic light scattering – a review. *Opt Laser Technol* 22:175–187
19. Goldburg WI (1999) Dynamic light scattering. *Am J Phys* 67:1152–1160